2006

Ferroelectricity Induced by Incommensurate Magnetism (Invited)

A. Brooks Harris
University of Pennsylvania, harris@sas.upenn.edu

Ferroelectricity Induced by Incommensurate Magnetism (Invited)

Abstract

Ferroelectricity has been found to occur in several insulating systems, such as $TbMnO_3$ and $Ni_3V_2O_8$ which have more than one phase with incommensurately modulated long-range magnetic order. Here we give a phenomenological model which relates the symmetries of the magnetic structure as obtained from neutron diffraction to the development and orientation of a spontaneous ferroelectric moment induced by the magnetic ordering. This model leads directly to the formulation of a microscopic spin-phonon interaction which explains the observed phenomena. The results are given in terms of gradients of the exchange tensor with respect to generalized displacements for the specific example of NVO. It is assumed that these gradients will now be the target of first-principles calculations using the LDA+U or related schemes

Disciplines
Physics | Quantum Physics

Ferroelectricity induced by incommensurate magnetism (invited)

A. Brooks Harris[a)]

Department of Physics and Astronomy, University of Pennsylvania, Philadelphia, Pennsylvania 19104

Ferroelectricity has been found to occur in several insulating systems, such as $TbMnO_3$ and $Ni_3V_2O_8$ which have more than one phase with incommensurately modulated long-range magnetic order. Here we give a phenomenological model which relates the symmetries of the magnetic structure as obtained from neutron diffraction to the development and orientation of a spontaneous ferroelectric moment induced by the magnetic ordering. This model leads directly to the formulation of a microscopic spin-phonon interaction which explains the observed phenomena. The results are given in terms of gradients of the exchange tensor with respect to generalized displacements for the specific example of NVO. It is assumed that these gradients will now be the target of first-principles calculations using the LDA+U or related schemes. © *2006 American Institute of Physics.* [DOI: 10.1063/1.2177392]

I. INTRODUCTION

Recently studies have focused on a family of multiferroics which displays a phase transition in which there simultaneously develops long-range incommensurate magnetic and uniform ferroelectric order. The most detailed studies have been carried out on the system $Ni_3V_2O_8$ (NVO).[1–4] A similar analysis of $TbMnO_3$ (TMO) has also appeared.[5,6] (For a review of both systems see, see Ref. 7.) To illustrate the phenomenon we show in Fig. 1 the data for the spontaneous polarization as a function of applied *magnetic* field.

These data indicate a strong coupling between the magnetic order parameters and the polarization order parameters. To interpret the effect of this coupling, we reproduce in Fig. 2 the phase diagram as function of temperature T and magnetic field H applied along the crystal **a** and **c** axes. Here we show the three magnetic phases that occur for $T \geq 2$ K. The high and low temperature incommensurate (HTI and LTI) phases are two distinct incommensurate phases. A spontaneous polarization appears throughout the LTI phase but does not appear in the other phases. Thus, applying a strong enough H to cross the LTI-antiferromagnetic (AF) phase boundary will kill the spontaneous polarization for $\mathbf{H} \| \mathbf{c}$ or allow it for $\mathbf{H} \| \mathbf{a}$. Since this transition is discontinuous, the hysteresis shown in Fig. 1 is to be expected.

This phenomenon has been explained[3] on the basis of a phenomenological model which invokes a Landau expansion in terms of the order parameters describing the incommensurate magnetic order and the order parameter describing the uniform spontaneous polarization. Already from this treatment it was clear that a microscopic model would have to involve a trilinear interaction Hamiltonian proportional to the product of two spin variables and one displacement variable. Furthermore, the symmetry requirements of the phenomenological model would naturally be realized by a proper microscopic model. In this paper we summarize the symmetry analysis and briefly describe the microscopic formulation which underlies the symmetry analysis.

II. THEORETICAL LEVELS

Since the initial theoretical interpretations of ferroelectricity induced by incommensurate magnetism[3] involved phenomenological arguments, it may be useful to review various levels at which theory can address this phenomenon. Clearly, the phenomenological level involves a description in terms of thermodynamic (i.e., classical commuting) variables, such as $M(\mathbf{q})$, the $\mathbf{q}$ Fourier component of the magnetic moment. As in thermodynamics, this approach does not specify the thermodynamic variables which are needed. Instead one identifies the lowest number of thermodynamic variables which leads to terms in a Landau-like expansion[3] which (a) describe order relative to the phase which is both paramagnetic and paraelectric and (b) explain how magnetically induced ferroelectricity can occur. As we shall discuss below, the appropriate thermodynamic variables are the Fourier amplitudes of the magnetization which transform according to the various irreducible representation of the group of the wave vector and the uniform polarization.

At the microscopic level, one can consider a Hubbard-like Hamiltonian which describes the interaction of the $3d$ electrons responsible for the Ni spins and the ionic displacements responsible for the spontaneous polarization. Here one needs as input a number of parameters such as Coulomb
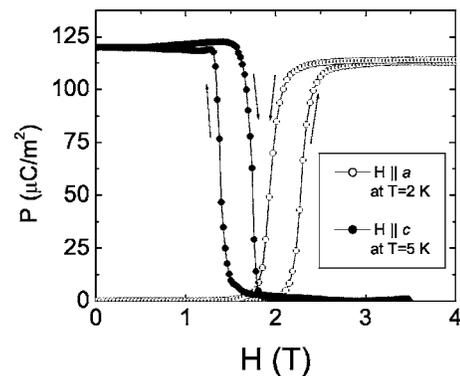

FIG. 1. Adapted from Ref. 3. Spontaneous polarization of NVO vs magnetic field applied along the **a** and **c** axes.

[a)]Electronic mail: harris@physics.upenn.edu
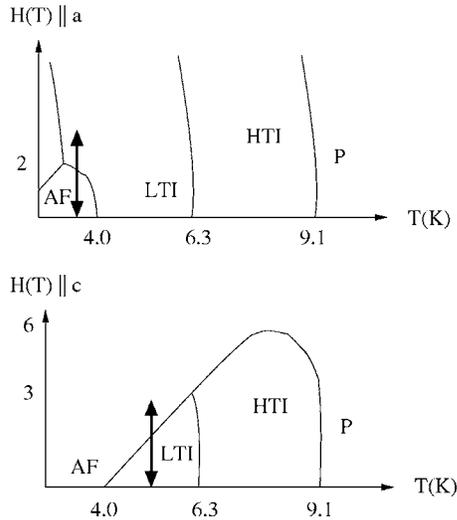
99, 08E303-1

FIG. 2. Adapted from Ref. 2. Phase diagram of NVO for magnetic fields up to 8 T applied along the **a** direction (top) and along the **c** direction (bottom). P (AF) denotes the paramagnetic (antiferromagnetic) phase. For $H \| \mathbf{c}$ there is no phase boundary between the P and AF phases. The arrowed vertical lines indicate the paths followed in Fig. 1.

integrals, spin-orbit coupling constants, and Hund's rule coupling constants which follow from atomic physics studies. Also, one needs the various hopping matrix elements and these are usually obtained from a calculation based on the local density approximation[8] (LDA) or possibly from a so-called LDA+U (Ref. 9) calculational scheme. In this Hubbard-like Hamiltonian it is illogical to include spin-spin interactions such as Heisenberg exchange or Dzialoshinskii-Moriya (DM) interactions.[10,11]

There is a level of detail which is intermediate between this microscopic Hubbard-like Hamiltonian and the phenomenological Landau expansion. At this intermediate level one studies the "low energy" Hamiltonian obtained from the Hubbard-like Hamiltonian by using a canonical transformation to eliminate the explicit appearance of high energy states, such as states which involve more Coulomb energy than the ground state. For most high-symmetry insulators this intermediate level involves consideration of an isotropic Heisenberg Hamiltonian for quantum spin operators, as originally discussed by Anderson.[12] In the case of NVO we expect that when states which violate Hund's rule are eliminated, we will obtain a spin Hamiltonian (for spin $S=1$) which is like the Heisenberg Hamiltonian, except that all anisotropic exchange interactions consistent with crystal symmetry (such as DM interactions) appear and, since we wish to treat ferroelectricity, ionic displacements also appear. In the present paper our aim is to first present an accessible exposition of the phenomenological approach and secondly to deduce from this approach the form of the Heisenberg-like low energy Hamiltonian. Normally, one cannot uniquely construct the intermediate level spin Hamiltonian solely from the phenomenological formulation. Here this is possible only because the phenomenological trilinear interaction involving two powers of $M(\mathbf{q})$ and the spontaneous polarization are uniquely related to a term in the spin Hamiltonian involving two powers of spin variables and one phonon displacement variable. However, the actual values of the coupling con-
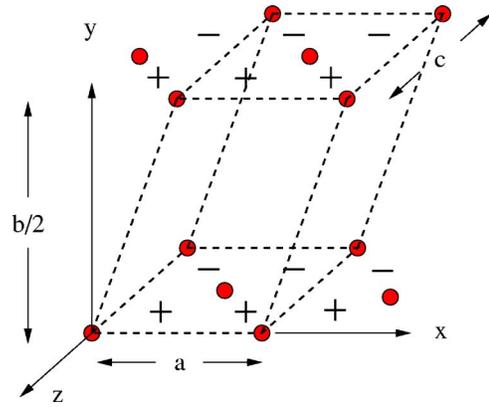

FIG. 3. Positions in NVO of Ni crosstie sites (filled circles) and Ni spine sites (indicated by + and − signs according to whether their y coordinate is larger than or less than that of the layer). The dashed lines outline the primitive unit cell.

stants in this low energy Hamiltonian can only be obtained from the Hubbard-like Hamiltonian which we are presently analyzing.

III. SYMMETRY OF THE MAGNETIC PHASES

We first discuss the crystal structure of NVO. The orthorhombic space group of NVO is $Cmca$ (No. 62 in Ref. 13). Apart from the primitive translations $\mathbf{a}_1 = (a/2)\hat{i} + (b/2)\hat{j}$, $\mathbf{a}_2 = (a/2)\hat{i} - (b/2)\hat{j}$, and $\mathbf{a}_3 = c\hat{k}$, the generators of the space group may be taken to be 2_x, a twofold rotation about the x axis, m_x, a reflection taking x into $-x$, and m_z, a glide plane which takes z into $-z$, followed by a translation of $(b/2)\hat{j} + (c/2)\hat{k}$. (As we will see below, invariance under spatial inversion $\mathcal{I} \equiv 2_x m_x$ plays a crucial role in our symmetry analysis.) The primitive unit cell contains two formula units of NVO and the magnetism is due to the Ni ions (see Fig. 3). There are two crystallographically inequivalent Ni sites which we will refer to as "spine" and "crosstie" sites. The positions of the spine sites within the unit cell are $\mathbf{r}_1 = (a/4, d, c/4)$, $\mathbf{r}_2 = (a/4, -d, c/4)$, $\mathbf{r}_3 = (3a/4, -d, 3c/4)$, and $\mathbf{r}_4 = (3a/4, d, c/4)$. The parameter $d \approx 0.13b$ indicates that the a-c planes are buckled kagomélike planes. The crosstie sites within the unit cell are at $\mathbf{r}_5 = (0,0,0)$ and $\mathbf{r}_6 = (a/2, 0, c/2)$.

The Ni spins form weakly coupled chains (or spines) parallel to the **a** axis. The nearest neighbor (nn) and next-nearest neighbor (nnn) exchange interactions along the spine (respectively, J_1 and J_2) compete with one another because, as shown in Fig. 4, in contrast to the situation in the cuprates, in the vanadates the nn interaction is anomalously weak. A result of this competition is that the spins order in an incommensurate state whose wave vector q along the **a** axis is given by[15]

$$\cos(aq/2) = -J_1/(4J_2), \qquad (1)$$

where an experiment[2] shows that $q \approx 0.28(2\pi/a)$.

The above description of the incommensurate phases is too simplistic. Accordingly we now turn to a more detailed discussion which takes proper account of the structure within
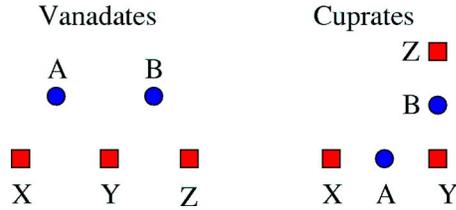
FIG. 4. First and second neighbor exchange paths (respectively, X-A-Y or Y-B-Z and X-A-B-Z) in the vanadates (Ref. 1) (left) and cuprates (right), where A and B are oxygen ions and X, Y, and Z are magnetic ions. In the vanadates the first neighbor exchange path is nearly a 90° path, so that the nn exchange is weak, whereas in the cuprates the path is a 180 path, so that here $J_2/J_1 \sim 0.1$ (see Ref. 14), whereas for the vanadates J_2/J_1 is much larger.[4]

each unit cell. The α component of the spin order at position $\mathbf{R}$ (which is the τth site in the unit cell) is expressed in terms of Fourier components at wave vector q as

$$S_{\alpha\tau}(\mathbf{R}) = [S_{\alpha\tau}(\mathbf{q})e^{i\mathbf{q}\cdot\mathbf{R}} + S_{\alpha\tau}(\mathbf{q})^* e^{-i\mathbf{q}\cdot\mathbf{R}}]/2, \quad (2)$$

where $S_{\alpha\tau}(\mathbf{q})$ is a complex-valued Fourier coefficient and $S_{\alpha\tau}(-\mathbf{q}) = S_{\alpha\tau}(\mathbf{q})^*$. Assuming that only a single Fourier wave vector condenses, we see that the spin structure is characterized by the six vector Fourier components of the unit cell. Since these quantities are three component vectors and each components is complex valued, this structure is characterized by 36 real-valued parameters. Translational invariance indicates that the Landau expansion of the free energy at quadratic order in terms of these Fourier components must assume the form

$$F_2 = \sum_{\mathbf{q}} F_2(\mathbf{q}), \quad (3)$$

where

$$F_2(\mathbf{q}) = \sum_{\alpha\alpha';\tau\tau'} c_{\alpha\tau,\alpha'\tau';\mathbf{q}} S_{\alpha\tau}(-\mathbf{q}) S_{\alpha'\tau'}(\mathbf{q}). \quad (4)$$

As we shall see, the use of symmetry drastically reduces the number of parameters needed to characterize the magnetic structure.

We now analyze the magnetic symmetry of NVO. Since the wave vector lies along the x axis, the free energy $F_2(\mathbf{q})$ must be invariant under the operations of the crystal which leave the x axis invariant. The group of these symmetry operations includes the identity operation $\mathcal{E}$, a twofold rotation about the x axis, 2_x, the glide reflection through a z plane, m_z, and $2_x m_z$. The pattern into which the spins order is determined by the eigenvector of $F_2(\mathbf{q})$ corresponding to the eigenvalue which first becomes negative as the temperature is reduced. This eigenvector must also be an eigenvector of the operation 2_x (with eigenvalue of either +1 or −1) and also of m_z (with eigenvalue of either +1 and −1). Thus the structure determination is much simplified. Instead of having to determine the six complex vectors $\mathbf{S}_n$ in the unit cell, we use the fact that these spin components form a vector which is simultaneously an eigenvector of $F_2(\mathbf{q})$, 2_x, and m_z. Accordingly we may specify (or guess) the four possible sets of eigenvalues of 2_x and m_z. This set of eigenvalues is technically known as the *irreducible representation* Γ or irrep for short. The actual active irrep is selected as the one which
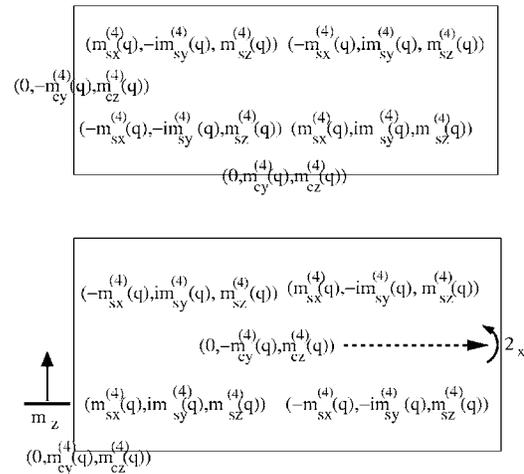

FIG. 5. Two adjacent $x-z$ planes in NVO (buckling not shown) showing Fourier coefficients $S_{\alpha\tau}(q)$ in terms of symmetry adapted parameters $\mathbf{m}^{(4)}(q)$ for the HTI irrep $\Gamma = \Gamma_4$, for which the eigenvalues of 2_x and m_z are −1 and +1, respectively. Here 2_x is the twofold axis about x and m_z is a glide plane which consists of a mirror plane shown at $z = c/4$ [which, because $\mathbf{m}(q)$ is a pseudovector, does not change the sign of $m_z(q)$ but does change the signs of $m_x(q)$ and $m_y(q)$] followed by a displacement $b/2$ along y (from one plane to the next).

best fits the diffraction data. For the HTI phase the active irrep is Γ_4 for which the eigenvalues of 2_x and m_z are −1 and +1, respectively.[2] For this irrep we have to specify the three complex spin amplitudes of a single spine site and the y and z components of a single crosstie site. The other amplitudes are then determined by application of the symmetry operators 2_x and m_z. Since we reject accidental degeneracy, the ordering of the HTI phase can only involve a single irrep. In Fig. 5, we show the spin function for the HTI phase of NVO corresponding to the eigenvalues of 2_x and m_z, respectively, −1 and +1, of irrep Γ_4.[2] Notice that the characterization of the magnetic structure requires the specification of only five complex-valued *symmetry adapted coordinates*, $m_{s\alpha}^{(4)}(q)$ and $m_{c\alpha}^{(4)}(q)$.

When the LTI phase is entered, the situation is much the same. In addition to a spin function with HTI symmetry, an additional ordering with a different symmetry develops. This additional symmetry is found to correspond to the eigenvalues of 2_x and m_z, respectively, +1 and +1 (of irrep Γ_1), and the corresponding spin functions (which require the specification of four additional symmetry adapted coordinates) $m_{s\alpha}^{(3)}(q)$ and $m_{c\alpha}^{(3)}(q)$ are shown in Fig. 6.

The crystal NVO is invariant under spatial inversion $\mathcal{I}$ and we have not yet discussed how this affects the analysis. Since spin is a pseudovector, inversion does not change the orientation of the spin but takes it into the spatially inverted position and therefore takes q into $-q$ (which is the same as complex conjugation). Also inversion takes the site $\mathbf{r}_1$ in the unit cell into site $\mathbf{r}_3$ and site $\mathbf{r}_2$ into site $\mathbf{r}_4$. Referring to Figs. 5 and 6, one sees that we have defined the spin components $m_{s\alpha}^{(n)}$ with appropriate phase factors of i so that

$$\mathcal{I}m_{s\alpha}^{(n)} = m_{s\alpha}^{(n)*}. \quad (5)$$

Including phase factors (of i) in Fig. 5 or 6 is at our convenience. If the system wanted the y components of the spin
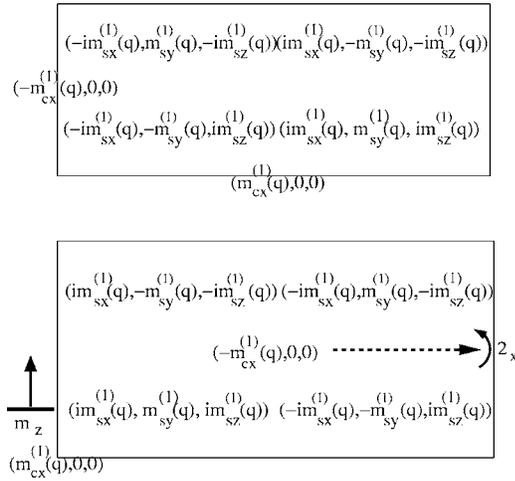
$(-im_{sx}^{(1)}(q),m_{sy}^{(1)}(q),-im_{sz}^{(1)}(q))(im_{sx}^{(1)}(q),-m_{sy}^{(1)}(q),-im_{sz}^{(1)}(q))$

$(-m_{cx}^{(1)}(q),0,0)$

$(-im_{sx}^{(1)}(q),-m_{sy}^{(1)}(q),im_{sz}^{(1)}(q))(im_{sx}^{(1)}(q),m_{sy}^{(1)}(q),im_{sz}^{(1)}(q))$

$(m_{cx}^{(1)}(q),0,0)$

$(im_{sx}^{(1)}(q),-m_{sy}^{(1)}(q),-im_{sz}^{(1)}(q))(-im_{sx}^{(1)}(q),m_{sy}^{(1)}(q),-im_{sz}^{(1)}(q))$

$(-m_{cx}^{(1)}(q),0,0)$ - - - - - - - - ⟶ 2_x

$(im_{sx}^{(1)}(q),m_{sy}^{(1)}(q),im_{sz}^{(1)}(q))(-im_{sx}^{(1)}(q),-m_{sy}^{(1)}(q),im_{sz}^{(1)}(q))$

m_z

$(m_{cx}^{(1)}(q),0,0)$

FIG. 6. As in Fig. 5 showing Fourier coefficients $S_{\alpha\tau}(q)$ in terms of symmetry adapted parameters for the LTI irrep $\Gamma=\Gamma_1$, for which the eigenvalues of 2_x and m_z are both +1.

moments to be in phase with the x components and if $m_{sx}(q)$ were real valued, then $m_{sy}(q)$ would be pure imaginary.

This same relation also holds for the crosstie order parameters without the necessity of introducing phase factors. Now consider the expansion of the free energy in terms of these variables, where for notational convenience we set (for each irreducible representation) $\xi_1(q)=m_{sx}(q)$, $\xi_2(q)=m_{sy}(q)$, $\xi_3(q)=m_{sy}(q)$, and $\xi_4(q)$, and if needed, $\xi_5(q)$ are similar crosstie order parameters. In terms of these variables the quadratic free energy is

$$F_2(\mathbf{q}) = \sum_{n,n';\Gamma} c_{n,n'}^{\Gamma} \xi_n^{\Gamma}(q)^* \xi_{n'}^{\Gamma}(q), \tag{6}$$

where the superscript identifies the irreducible representation. To ensure the reality of $F_2(\mathbf{q})$ we must have $c_{n',n}^{\Gamma}=c_{n,n'}^{\Gamma *}$. Equation (5) implies that

$$\mathcal{I}\xi_n^{\Gamma}(q) = \xi_n^{\Gamma}(q)^*. \tag{7}$$

Now for $F_2(\mathbf{q})$ to be invariant under $\mathcal{I}$ we must have

$$\mathcal{I}\mathcal{F}_2(\mathbf{q}) = \sum_{n,n';\Gamma} c_{n,n'}^{\Gamma}[\mathcal{I}\xi_n^{\Gamma}(q)^*][\mathcal{I}\xi_{n'}^{\Gamma}(q)]$$

$$= \sum_{n,n'} c_{n,n'}^{\Gamma}\xi_n^{\Gamma}(q)\xi_{n'}^{\Gamma}(q)^* = F_2(\mathbf{q}). \tag{8}$$

This indicates that $c_{n,n'}^{\Gamma}=c_{n'n}^{\Gamma}$, which together with $c_{n',n}^{\Gamma}=c_{n,n'}^{\Gamma}(q)^*$ means that all the coefficients $c_{n,n'}^{\Gamma}$ are real valued. This means that apart from an overall phase factor, all the components of the eigenvector are real. So for each representation Γ, we write

$$\xi_n^{\Gamma}(q) = \sigma_{\Gamma}e^{i\phi_{\Gamma}}r_n^{\Gamma}, \tag{9}$$

where the r_n^{Γ} are the components of a real-valued unit vector. This result indicates that the $m_{s\alpha}$'s of a given representation all have the same phase. Some of the spine spin components are proportional to $im_{s\alpha}$, and such spine spin components are 90° out of phase from those which do not have the factor i. Accordingly, since both $m_{sx}^{(4)}(q)$ and $m_{sy}^{(4)}(q)$ are nonzero,[2] the spin structure of a single spine in the HTI phase is actually a

spin spiral. The HTI phase has inversion symmetry because one spiral in the unit cell is the inverted image of the other spiral in the unit cell.

Instead of giving the representation Γ as a script on the ξ's, ϕ's, and r's, we will write HTI (for Γ_4) or LTI (for Γ_1). By writing the symmetry adapted coordinates in the form of Eq. (9), one sees that this type of incommensurate ordering is characterized by an $x-y$-like order parameter $\boldsymbol{\sigma}_{\Gamma}(q) \equiv \sigma_{\Gamma}\exp(i\phi_{\Gamma})$ which has a magnitude σ_{Γ} and a phase ϕ_{Γ}. The magnitude of the order parameters σ_{Γ} is fixed by terms (we have not considered) which are fourth order in the spin components. These and higher order terms have no effect on the normalized eigenvector as long as one is close to the ordering transition. From Eq. (7) we see that for each representation

$$\mathcal{I}\sigma_{\Gamma} = \sigma_{\Gamma}, \quad \mathcal{I}\phi_{\Gamma} = -\phi_{\Gamma}. \tag{10}$$

Apart from the overall phase, the spin structure of the HTI phase is specified by the wave vector q and the five real-valued parameters r_n^{HTI}, and the additional ordering appearing in the LTI phase requires specifying four real-valued parameters r_n^{LTI} and the relative phase $\phi_{\mathrm{LTI}}-\phi_{\mathrm{HTI}}$.

IV. MAGNETOELECTRIC COUPLING: PHENOMENOLOGY

In Ref. 3 it was proposed that one could understand the magnetically induced ferroelectricity in terms of the following Landau expansion:

$$F = F_M + \frac{1}{2\chi_E}\mathbf{P}^2 + V_{\mathrm{int}}, \tag{11}$$

where F_M is the free energy of the system in the absence of a nonzero polarization [and which is given up to quadratic order by $F_2(\mathbf{q})$], $\mathbf{P}$ is the uniform electric polarization, and χ_E is the electric susceptibility, which we assume to be finite since we assume that when the magnetism is absent the spontaneous polarization is zero. Here V_{int} is the magnetoelectric interaction which is posited to be of the form

$$V_{\mathrm{int}} = \sum_{\alpha\beta\gamma} c_{\alpha\tau,\beta\tau'}(\mathbf{q})S_{\alpha\tau}(-\mathbf{q})S_{\beta\tau'}(\mathbf{q})P_{\gamma}, \tag{12}$$

where γ labels the Cartesian components of $\mathbf{P}$. This interaction may be viewed as that of an effective electric field proportional to a quadratic combination of spin variables and which thereby induces a nonzero polarization only when the magnetic order parameters are nonzero. Because the spin components are expressible in terms of the $x-y$-like order parameters introduced in Eq. (9), we may write this as

$$V_{\mathrm{int}} = \sum_{AB\gamma} c_{AB\gamma}(\mathbf{q})\boldsymbol{\sigma}_A(q)\boldsymbol{\sigma}_B(-q)P_{\gamma}, \tag{13}$$

where A and B are summed over the values HTI and LTI. In the HTI phase the LTI order parameter is zero, so that

$$V_{\mathrm{int}} = \sum_{\gamma} c_{\mathrm{HTI,HTI},\gamma}(q)|\boldsymbol{\sigma}_{\mathrm{HTI}}(q)|^2 P_{\gamma}. \tag{14}$$

But since this interaction has to be inversion invariant, the coefficient $c_{\mathrm{HIT,HTI},\gamma}(q)$ must vanish. Thus symmetry does

not allow a spontaneous polarization to be induced by magnetic ordering in the HTI phase. A simple (but not rigorous) way to reach this conclusion is to observe that the phase of an incommensurate wave will vanish arbitrarily close to some crosstie site. If one then takes this site as the origin, the magnetic structure will have inversion symmetry relative to this new origin and hence a spontaneous polarization is not allowed. We should also remark that it is not strictly accurate to correlate the existence of ferroelectricity with a magnetic spiral. As we remarked just below Eq. (9), the magnetic structure of the HTI phase has a small nonzero y component of spin, so that the unit cell contains two spirals which are arranged in such a way that the HTI phase has a center of inversion symmetry. So the loose statement that ferroelectricity arises from a spiral magnetic structure is not completely accurate.

In the LTI phase the situation is different. Although the term involving $|\sigma_{\mathrm{LTI}}|^2$ vanishes by the above argument, one has

$$V_{\mathrm{int}} = \sum_{\gamma} P_{\gamma}[c_{\gamma}(q)\boldsymbol{\sigma}_{\mathrm{HTI}}(q)\boldsymbol{\sigma}_{\mathrm{LTI}}(q)^{*}$$
$$+ c_{\gamma}(q)^{*}\boldsymbol{\sigma}_{\mathrm{HTI}}(q)^{*}\boldsymbol{\sigma}_{\mathrm{LTI}}(q)]. \tag{15}$$

Using Eq. (10) one sees that for this to be invariant under spatial inversion the coefficient $c_{\gamma}(q)$ has to be pure imaginary, so that V_{int} has to be of the form

$$V_{\mathrm{int}} = \sum_{\gamma} r_{\gamma}\sigma_{\mathrm{HTI}}\sigma_{\mathrm{LTI}}\sin(\phi_{\mathrm{LTI}} - \phi_{\mathrm{HTI}})P_{\gamma}, \tag{16}$$

where r_{γ} is real valued. Thus a requirement that for NVO incommensurate magnetic order induce a spontaneous polarization is that the two order parameters $\boldsymbol{\sigma}_{\mathrm{HTI}}$ and $\boldsymbol{\sigma}_{\mathrm{LTI}}$ should not be in phase, i.e., $\phi_{\mathrm{HTI}} \neq \phi_{\mathrm{LTI}}$. An analysis[16] of the fourth order terms in the Landau expansion of F_M indicates that indeed these two order parameters do not have the same phase. We now consider the effect of the symmetries 2_x and m_z. From the symmetries of the active irreps (or from inspection of Figs. 5 and 6), one can see that

$$2_x[\boldsymbol{\sigma}_{\mathrm{HTI}}\boldsymbol{\sigma}_{\mathrm{LTI}}^{*}] = -[\boldsymbol{\sigma}_{\mathrm{HTI}}\boldsymbol{\sigma}_{\mathrm{LTI}}^{*}] \tag{17}$$

and

$$m_z[\boldsymbol{\sigma}_{\mathrm{HTI}}\boldsymbol{\sigma}_{\mathrm{LTI}}^{*}] = [\boldsymbol{\sigma}_{\mathrm{HTI}}\boldsymbol{\sigma}_{\mathrm{LTI}}^{*}]. \tag{18}$$

But the product $P_{\gamma}\boldsymbol{\sigma}_{\mathrm{HTI}}\boldsymbol{\sigma}_{\mathrm{LTI}}^{*}$ must be invariant under these two symmetry operations. Thus P_{γ} must change sign under 2_x but be invariant under m_z. This implies that **P** can only have a nonzero component along **b**, as is observed.[3]

To summarize, the Landau symmetry analysis for NVO explains why ferroelectricity can only be induced in the LTI phase which is described by two different symmetry order parameters. (This is reminiscent of the analysis of the symmetry of second harmonic generation.[17]) In addition this symmetry analysis correctly predicts that incommensurate magnetic order can only induce a spontaneous polarization along the crystallographic **b** direction. A completely similar analysis has been developed[6] for TbMnO$_3$ which exhibits a similar magnetically induced ferroelectricity.[5]
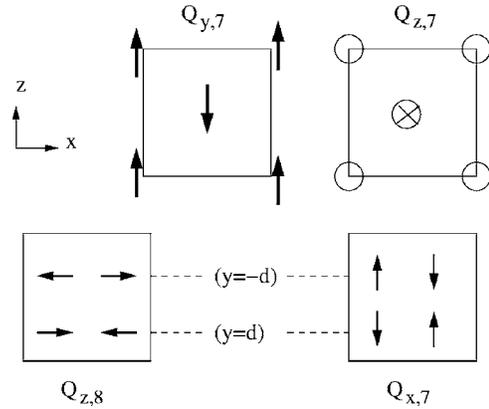

FIG. 7. Adapted from Ref. 19. Top: generalized displacements of crosstie Ni atoms which transform like y (left) and like z (right). Plain circles represent displacements out of the page and a circle with a cross represents a displacement into the page. Bottom: generalized displacements of Ni spine atoms which transform like z (left) and like x (right).

V. MAGNETOELECTRIC COUPLING: MICROSCOPICS

As noted in Ref. 3 and mentioned above, the form of the trilinear magnetoelectric coupling of Eq. (12) leads directly to the construction of a microscopic spin Hamiltonian which must underlie the symmetry analysis presented above. Since a polarization can only come from a displacement of the effective ionic charge (e.g., see Ref. 18), the microscopic interaction must involve the coupling of two spin operators and one displacement operator. The generalized exchange tensor interaction between spins at sites i and j is

$$\mathcal{H}(i,j) = \sum_{\alpha\beta} J_{\alpha\beta}(i,j)S_{\alpha}(i)S_{\beta}(j). \tag{19}$$

Here we allow for both symmetric and antisymmetric (DM) interactions.[10,11] To get a displacement operator, we simply expand the exchange tensor **J** up to first order in the atomic displacements. Note that a uniform polarization must arise from a zero wave vector optical phonon. Although the energies and wave functions of the optical phonons are unknown, they must be linear combinations of the symmetry adapted zero wave vector generalized displacements (GDs) and we express our results in terms of these GDs. We only need to consider GDs which transform like a vector under the symmetry operations of the crystal, because only these GDs can carry a dipole moment. These GDs are denoted $Q_{\alpha n}$, where α labels the component x, y, or z according to which Q transforms. Some of these GDs are easy to construct: A GD in which all crystallographically equivalent atoms, e.g., Ni spines, Ni crossties, or V ions, move along the same crystallographic direction α will generate the $Q_{\alpha,n}$'s for $n \leq 6$, because NVO has six crystallographically inequivalent sites. The other relevant GDs are given elsewhere,[7,19] but we show a few of these in Fig. 7. To verify the symmetry of the GDs shown here, it is useful to consider the effect of 2_x, m_x, and 2_y, which is a twofold rotation about a y axis passing through a spine site. For instance, consider the effect of these operations on $Q_{z,8}$. This GD is odd under 2_x (a twofold rotation about the center of the cell), even under m_x, and is odd under 2_y. These evaluations verify that this GD does have the same symmetry as a z coordinate. This means that, perhaps sur-

prisingly, this mode gives rise to a dipole moment in the z direction. One can also see that $Q_{z,8}$ couples to the GD in which all the crossties move in parallel along the z axis. Suppose the atom-atom potential is repulsive. Then when the spine atoms move as shown in Fig. 7, they force the crosstie (not shown) at the center of the unit cell to move towards negative y and positive z and the crosstie (not shown) at the corner of the unit cell to move towards positive y and positive z. Thus $Q_{z,8}$ couples to a uniform displacement of the crosstie along the z axis, as its symmetry label indicates. The most important GDs are the $Q_{\alpha,n}$ for $n \leqslant 6$ since their dipole moments are expected to be the largest.

In this development the spin-phonon coupling involves the various derivatives

$$J_{\alpha\beta}^{\gamma_n} \equiv \frac{\partial J_{\alpha\beta}}{\partial Q_{\gamma_n}}. \qquad (20)$$

The algebra needed to construct the spin-phonon Hamiltonian $\mathcal{H}_{s\text{-}p}$ when the spin operators are replaced by their thermal averages is straightforward but tedious and is given elsewhere when nn spine-spine, spine-crosstie, as well as second neighbor spine-spine interactions are taken into account.[7,19] Only terms which involve $Q_{\alpha,n}$ with $\alpha = y$ are nonzero, in agreement with the macroscopic symmetry analysis.[3] To illustrate the results of these calculations, we give here the result for nn spine-spine interactions,[7,19]

$$\mathcal{H}_{s\text{-}p} = 16 N_{\text{uc}} \sum_p Q_{y_p} \sum_{\mu,\nu=x,y,z} \Lambda_{\mu\nu}^{(nn)} \mathfrak{I}[m_{s,\mu}^{(4)}(q)^* m_{s,\nu}^{(1)}(q)], \quad (21)$$

where N_{uc} is the number of unit cells, $\mathfrak{I}$ indicates the imaginary part, and

$$\mathbf{\Lambda}^{(nn)} = \begin{bmatrix} J_{xx}^{y_p}c & D_z^{y_p}s & D_y^{y_p}c \\ -D_z^{y_p}s & -J_{yy}^{y_p}c & -J_{yz}^{y_p}s \\ D_y^{y_p}c & J_{yz}^{y_p}s & -J_{zz}^{y_p}c \end{bmatrix}, \qquad (22)$$

where $c \equiv \cos(qa/2)$, $s \equiv \sin(qa/2)$, $J_{\alpha\beta}$ is the symmetric part of the nn spine-spine exchange tensor, and $\mathbf{D}$ is the associated Dzialoshinskii-Moriya vector. Note that this result explicitly requires two irreps, also in accord with the macroscopic symmetry analysis. [The terms in Eq. (21) involving a single irrep were evaluated to be zero.] It should also be noted that due to the low site symmetry, the spin-phonon coupling involves the derivatives of almost all elements of the generalized exchange tensor. In principle, one should also consider higher order interactions, such as four spin terms, but for simplicity we ignore these at the moment. The next step (which is ongoing) is to evaluate the necessary gradients of the exchange tensor from a first-principles calculation based on a Hubbard-like Hamiltonian and to incor-
porate the mode structure and energy of the optical modes at zero wave vector.

VI. SUMMARY

In this paper I have reviewed the symmetry analysis of the interaction responsible of ferroelectricity in $Ni_3V_2O_8$ induced by incommensurate magnetism[3] and have also summarized some results of the corresponding microscopic theory.[7,19] The key result is that ferroelectricity can only be magnetically induced in orthorhombic inversion symmetric lattices by the simultaneous existence of two distinct magnetic representations, in other words, two distinct types of coexisting magnetic symmetry. As we noted just below Eq. (9), it is not entirely accurate to correlate the existence of ferroelectricity with the existence of a spiral magnetic structure. This symmetry analysis has also recently been applied to some of the phases of $TbMO_3$.[6] It seems likely that these approaches will prove useful for a number of other multiferroics.

[1] N. Rogado, G. Lawes, D. A. Huse, A. P. Ramirez, and R. J. Cava, Solid State Commun. **124**, 229 (2002).
[2] G. Lawes *et al.*, Phys. Rev. Lett. **93**, 247201 (2004).
[3] G. Lawes *et al.*, Phys. Rev. Lett. **95**, 087205 (2005).
[4] M. Kenzelmann *et al.*, e-print cond-mat/0510386.
[5] N. Hur, S. Park, P. A. Sharma, J. S. Ahn, S. Guha, and S.-W. Cheong, Nature (London) **429**, 392 (2004).
[6] M. Kenzelmann *et al.*, Phys. Rev. Lett. **95**, 087206 (2005).
[7] A. B. Harris and G. Lawes, *The Handbook of Magnetism and Advanced Magnetic Materials* (Wiley, London, 2006), e-print cond-mat/0508617.
[8] P. C. Hohenberg and W. Kohn, Phys. Rev. **136**, B864 (1964); W. Kohn and L. J. Sham, *ibid.* **140**, A1133 (1965).
[9] V. I. Anisimov, F. Aryasetiawan, and A. I. Lichtenstein, J. Phys.: Condens. Matter **9**, 767 (1997).
[10] I. Dzyaloshinskii, J. Phys. Chem. Solids **4**, 241 (1958).
[11] T. Moriya, Phys. Rev. **120**, 91 (1960).
[12] P. W. Anderson, Phys. Rev. **115**, 2 (1959).
[13] A. J. C. Wilson, *International Tables For Crystallography* (Kluwer Academic, Dordrecht, 1995), Vol. A.
[14] Y. J. Kim *et al.*, Phys. Rev. B **64**, 024435 (2001).
[15] T. Nagamiya, in *Solid State Physics*, edited by F. Seitz and D. Turnbull (Academic, New York, 1967), Vol. 29, p. 346.
[16] A. B. Harris, A. Aharony, O. Entin-Wohlman, T. Yildirim, and M. Kenzelmann (unpublished).
[17] D. Frohlich, St. Leute, V. V. Pavlov, and R. V. Pisarev, Phys. Rev. Lett. **81**, 3239 (1998).
[18] J. H. M. van den Berg and A. van der Avoird, J. Phys.: Condens. Matter **1**, 4047 (1989).
[19] A. B. Harris, T. Yildirim, A. Aharony, and O. Entin-Wohlman, e-print cond-mat/0510807.